

# PuTR: A Pure Transformer for Decoupled and Online Multi-Object Tracking

Chongwei Liu<sup>1</sup> Haojie Li<sup>2\*</sup> Zhihui Wang<sup>1</sup> Rui Xu<sup>1</sup>

<sup>1</sup>Dalian University of Technology

<sup>2</sup>Shandong University of Science and Technology

lcwdllg@mail.dlut.edu.cn hjli@sdust.edu.cn

zhwang@dlut.edu.cn xurui@dlut.edu.cn

## Abstract

Recent advances in Multi-Object Tracking (MOT) have achieved remarkable success in short-term association within the decoupled tracking-by-detection online paradigm. However, long-term tracking still remains a challenging task. Although graph-based approaches can address this issue by modeling trajectories as a graph in the decoupled manner, their non-online nature poses obstacles for real-time applications. In this paper, we demonstrate that the trajectory graph is a directed acyclic graph, which can be represented by an object sequence arranged by frame and a binary adjacency matrix. It is a coincidence that the binary matrix matches the attention mask in the Transformer, and the object sequence serves exactly as a natural input sequence. Intuitively, we propose that a pure Transformer can naturally unify short- and long-term associations in a decoupled and online manner. Our experiments show that a classic Transformer architecture naturally suits the association problem and achieves a strong baseline compared to existing foundational methods across four datasets: DanceTrack, SportsMOT, MOT17, and MOT20, as well as superior generalizability in domain shift. Moreover, the decoupled property also enables efficient training and inference. This work pioneers a promising Transformer-based approach for the MOT task, and provides code to facilitate further research. <https://github.com/chongweiliu/PuTR>

## 1 Introduction

Multi-Object Tracking (MOT) is a fundamental yet challenging task, playing a pivotal role in modern perception systems for demanding applications like autonomous driving [17], video surveillance [16], and behavior analysis [21]. Over the decades, various methodologies, such as motion estimation [4; 57] or graph-based approaches [22; 5], have been exploited to tackle this problem, garnering significant attention.

Among them, the decoupled tracking-by-detection online paradigm has emerged as the dominant approach in recent years due to its simplicity and effectiveness. In this setting, detection results are obtained from a pre-trained detector (e.g., YOLOX [20]) and treated as immutable. Researchers then focus primarily on the association problem. Methods like SORT [4] or ByteTrack [57] exemplify this approach, exploiting motion cues via the Kalman filter [23] and associating objects based on the Hungarian algorithm [24], demonstrating impressive generalization ability in short-term tracking.

To simultaneously handle short- and long-term tracking challenges, methods such as MPNTrack [5] or SUSHI [10] model trajectories as a graph in the decoupled manner and leverage Graph Neural Networks (GNNs) [40] for association. These methods excel at maintaining tracklet completeness after long-range occlusions, with the only drawback being their non-online nature.

Consequently, an intriguing question arises: is it possible to unify short- and long-term tracking in a decoupled and online manner? We attempt to address this question in Fig.1. By observing the

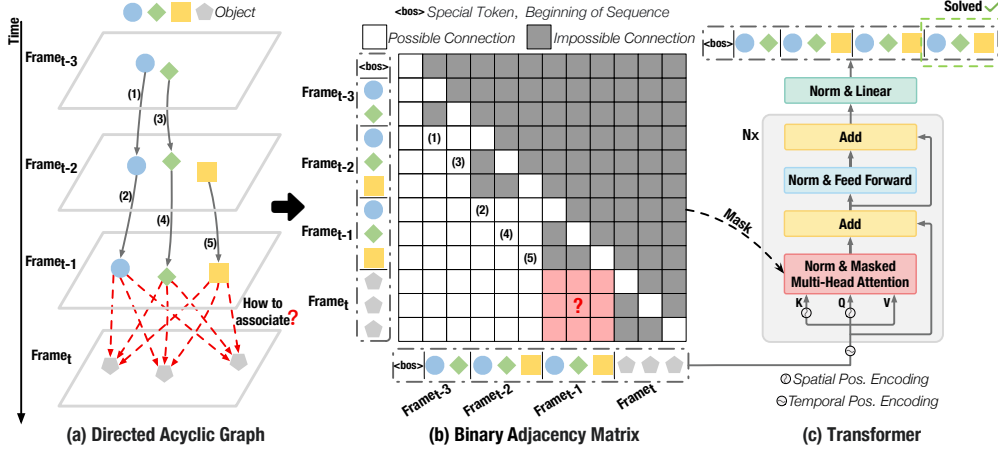


Figure 1: Illustration of our chain of thought. Trajectories are inherently a directed acyclic graph in the temporal order (a). We can thus transform it equivalently into a binary adjacency matrix (b), exactly aligning with the Transformer’s attention mask. Consequently, arranging objects by frame forms a natural input sequence for the Transformer (c), enabling it to model the association problem.

trajectory graph in Fig. 1a, we notice that each trajectory propagates independently along the temporal dimension, indicating that each object (node) has at most one in-degree and one out-degree. This implies that the trajectory graph is a strict directed acyclic graph, and its corresponding adjacency matrix is binary. Therefore, we can arrange objects by frame as a sequence and form a binary adjacency matrix to describe the trajectory graph, as shown in Fig. 1b. The binary matrix can be divided into white blocks representing possible connections (edges) and gray blocks representing impossible connections, where established trajectories will always lie within the white blocks. Due to the causality of trajectories in the frame sequence and forbidden connections among objects within the same frame, the white blocks exhibit an approximate lower triangular structure, formally aligned with the attention mask in the Transformer [46], while the object sequence serves exactly as a natural input sequence, as shown in Fig. 1c. This coincidence suggests an intuitive idea: directly applying a pure Transformer for association in a decoupled and online fashion.

While this idea seems straightforward, has there been any research already introducing the Transformer structure into MOT? The answer is yes, and no. Yes, because the pioneering works TrackFormer [31] and MOTR [54] have introduced the Transformer-based object detector DETR [9] into MOT in an end-to-end manner. They modify Deformable-DETR [61] to treat a tracklet as a hidden state in a query token and propagate it across frames to perform detection and association simultaneously. This inherent propagation gene is derived from earlier works like Tracktor [2] or CenterTrack [59], where CNN detectors (Faster RCNN [36] or CenterNet [60]) were employed in that era. We therefore also say the answer is no, because track propagation is more akin to a Recurrent Neural Network (RNN) [39] instead of a Transformer - the true power of the self-attention mechanism to model long-range dependencies is not exploited in the association. *Our straightforward idea aims to take a small step forward in exploring the potential of a pure Transformer for the association problem of MOT, paving the way for another promising new research direction in this field.*

In this paper, we exploit a **Pure Transformer**, named PuTR, to validate our idea. PuTR leverages the basic Transformer architecture to address the association challenge uniformly, as Fig. 1c shows. We modify the attention mask and incorporate temporal and spatial positional encodings to adapt it to the unique characteristics of the object sequence compared to a normal text sequence. Specifically, unlike a sentence, the object sequence is ordered in the outer frame temporal dimension but unordered in the inner image spatial dimension. Therefore, we modify the attention mask to ensure permutation invariance within the same frame, and also introduce temporal and spatial positional encodings to encode the frame order and the object coordinate information into the object sequence. We conduct extensive experiments on four MOT datasets: DanceTrack [43], SportsMOT [11], MOT17 [32], and MOT20 [12], to demonstrate the effectiveness of our approach. The results show that PuTR achieves a strong baseline compared to existing foundational methods, indicating the potential of this new direction. Notably, PuTR exhibits superior generalizability in domain shift, i.e., without fine-tuning, the maximum cross-dataset gap is only 2.7% in IDF1 [37] and 2.3% in HOTA [29]. Furthermore,

PuTR is efficient both in training and inference. It can be trained from scratch on a single GPU in less than 1 hour without additional data or complex training processes, and achieves up to 90 FPS in inference when given detection results. We provide our code to facilitate other researchers in following and promoting this promising direction into a new phase.

## 2 Related Work

Over the years, researchers have exploited various methodologies to address the challenging association problem in MOT, leading to diverse approaches in this field. Here, we provide a concise overview of the most representative methodologies in MOT. Additionally, the MOT task can also be modeled using techniques such as unsupervised learning [26], trajectory forecasting [13], and deep reinforcement learning [47]; however, these are not covered here due to space limitations.

**Heuristic Methods.** These have been widely studied and remain the most prevalent paradigm in this field. In the decoupled approach, these methods first detect objects using pre-trained object detectors [36; 20; 60] in each frame, and then associate them across frames online. Motion and spatial proximity cues are central to these methods. The foundational method SORT [4] utilizes the Kalman filter to estimate object motion and the Hungarian algorithm for association, and introduces a run-time manager to dynamically schedule the tracklet states (tracked, lost, or new). Subsequent methods primarily focus on increasing the robustness of frame-by-frame object association by incorporating appearance cues via an independent ReID model [49; 15; 51], introducing a more sophisticated motion model [57; 8; 25], or leveraging camera motion compensation to handle camera movements [1; 30]. These methods achieve impressive performance in short-term tracking scenarios, while more ingenious hand-crafted rules are urgently needed to maintain tracklet completeness in long-term tracking scenarios.

**Graph-based Methods.** Another perspective is to model the MOT as a graph optimization problem. Also under the decoupled approach, these methods represent nodes as detected objects and edges as trajectory hypotheses. In contrast to the frame-by-frame trackers mentioned above, graph-based methods search for global solutions to the data association problem over several frames or even the entire video sequence. This allows them to be more robust in semi-online or offline settings. Initially, numerous optimization frameworks were studied, including minimizing fixed costs [22; 34; 55], multi-cuts [44], and minimum cliques [38]. Recently, GNN-based methods [5; 10] have shown promise as an alternative to traditional optimization methods. MPNTrack [5] introduces a message passing network to dissect information and associate detections through edge classification. Building upon it, SUSHI [10] uses multiple hierarchical levels recursively to further optimize the graph space overhead and extend the ability to process long videos. Under the global perspective, they can handle short- and long-term tracking challenges uniformly, while the results are obtained offline, limiting wider real-time applications. Based on the heuristic and graph-based methods, PuTR is constantly exploring a new direction to unify association in a decoupled and online manner.

**Detector-based Methods.** Since a ready-made object detector is a prerequisite for the tracking-by-detection paradigm, it is natural to consider integrating the detector and tracker into a unified framework. As a transitional form before unification, JDE [48] and FairMOT [58] propose modifying CNN-based detectors [35; 60] to generate object bounding boxes and appearance features simultaneously for heuristic association, termed Joint-Detection-and-Embedding (JDE). For the unified framework in the CNN era, Tracktor [2] and CenterTrack [59] modify CNN-based detectors [36; 60] to use the previous tracklet results to predict the current tracklet results, thereby merging them into trajectories. In the Transformer era, the DETR family [9; 61; 27] has become mainstream. TrackFormer [31] and MOTR [54] therefore first extended the object queries in Deformable-DETR to the MOT task, using queries to represent tracked objects and propagating them into the next frame. Subsequent methods primarily focus on introducing a memory bank to store historical object embeddings [7; 18] or resolving conflicts between newborn and tracked object queries [50; 53]. Although the base detector has evolved from CNN to Transformer, the core mechanism for handling tracklets remains the same, i.e., updating the hidden state of the tracklet by the current frame and then propagating it to the next in an RNN-style manner. Therefore, we suggest that PuTR explores another way of employing the Transformer to MOT, i.e., association - not detection.

More recently, MOTIP [19] has also realized the potential of the Transformer for association, formulating it as an end-to-end in-context ID prediction problem. It constructs a learnable ID dictionary and attaches a Transformer decoder behind Deformable-DETR to predict tracking IDs of current detections, using historical trajectories as  $K$  and  $V$ , and current detections as  $Q$  in the

attention mechanism. It seems we have discovered a similar idea, albeit PuTR operates in a decoupled manner akin to a pure decoder-only Transformer, allowing efficient single-GPU training without pre-training or complex stabilization techniques. In contrast, MOTIP’s end-to-end nature necessitates a more complicated training process involving substantial data and multiple GPUs (usually 8) to mitigate overfitting. Additionally, MOTIP’s ID dictionary requires empirical tuning of its size for different datasets and risks exhaustion when tracked objects exceed its capacity, whereas PuTR proposes to associate objects via relative affinity, circumventing such issues and achieving superior generalizability under domain shift.

Notably, we do not aim to replace the end-to-end methods. Each methodology does not exist in opposition; instead, there are connections among them. For instance, the run-time manager is also utilized in DETR-based methods, and our idea draws inspiration from the trajectory graph used in GNN-based approaches. On the spectrum of methodologies, MOTIP may be viewed as an intermediate form bridging MOTR and PuTR. Each method explores MOT in their respective ecological niches, introducing new diversity to the field. Indeed, we emphasize that with sufficient video-level training data (e.g., DanceTrack), these end-to-end frameworks outperform decoupled methods. Our decoupled approach serves as a baseline when video data is scarce (e.g., MOT17). We believe that different paradigms can coexist and complement each other, providing a more comprehensive solution to the MOT community.

### 3 Method

#### 3.1 Preliminary

**Problem Formulation.** We first introduce the fundamental concepts and notations used in PuTR. Our approach follows the tracking-by-detection paradigm. Given a video, we assume that object detections are computed for every frame, and our task is to perform data association by linking object detections into online trajectories.

We denote the set of objects in the  $t$ -th frame as  $\mathcal{O}_t = \{o_{tid}^t\}$ , where  $o_{tid}^t$  represents the detected object in the  $t$ -th frame with the tracking identity  $tid$ . Each  $o_{tid}^t$  is represented by its bounding box coordinates, confidence score, and category label. The tracking identity  $tid$  is assigned to each object belonging to the same trajectory, with  $tid = -1$  indicating that the object does not belong to any trajectory. Within an  $\mathcal{O}_t$  set, each  $tid$  is unique, except for  $-1$ . The goal of data association is to obtain the set of trajectories  $\mathcal{T}^*$  that group detections corresponding to the same identity. Each trajectory  $\mathcal{T}_k \in \mathcal{T}^*$  is given by its set of detections  $\mathcal{T}_k = \{o_k^t \mid t_{s,k} \leq t \leq t_{e,k}\}$ , where  $t_{s,k}$  and  $t_{e,k}$  are the start and end frames of the trajectory  $\mathcal{T}_k$ , respectively.

**Input Object Sequence.** Similar to Transformer [46], the input of PuTR is also a sequence, but consisting of object detections in recent  $T + 1$  consecutive frames. We denote the input object sequence as  $\mathcal{S} = (\langle \text{bos} \rangle, \mathcal{O}_{t-T}, \dots, \mathcal{O}_{t-1}, \mathcal{O}_t)$ . Following language models [6; 45], the sequence  $\mathcal{S}$  starts with a special token  $\langle \text{bos} \rangle$  to indicate the beginning of the sequence, which is an all-zero token. The input sequence is then fed into PuTR after tokenization.

**Tokenization.** To feed the object detections into PuTR, we first convert each object detection  $o_{tid}^t$  into a token representation. We denote the token representation of object  $o_{tid}^t$  as  $x_{tid}^t$  and the corresponding token set as  $\mathcal{X}_t = \{x_{tid}^t\}$  in the  $t$ -th frame. It is feasible to map objects into high-dimensional vectors by employing an independent Re-ID model [49] or DETR object embeddings [54]. However, in this work, we adopt a variant from ViT [14] to encode the objects, avoiding the introduction of additional complexity. Specifically, for each object image patch  $p_{tid}^t \in \mathbb{R}^{h \times w \times 3}$ , generated by cropping the corresponding object detection bounding box<sup>1</sup> from the  $t$ -th frame, we divide it into a  $64 \times 64$  grid and sample the center point of each grid via bilinear interpolation. We then flatten these points to obtain the one-dimensional representation  $r_{tid}^t \in \mathbb{R}^{(64 \times 64 \times 3)}$ , and pass it through a linear layer to obtain the tokenized representation  $x_{tid}^t$  with the same dimension as the PuTR dimension  $d_{\text{model}} = 512$ . The tokenized sequence thus becomes  $\mathcal{S}_{in} = (\langle \text{bos} \rangle, \mathcal{X}_{t-T}, \dots, \mathcal{X}_{t-1}, \mathcal{X}_t) \in \mathbb{R}^{n_S \times d_{\text{model}}}$ , where  $n_S$  is the token number of the sequence.

---

<sup>1</sup> $h$  and  $w$  are the height and width of the bounding box, respectively.

### 3.2 Architecture & Modifications

**Architecture.** As illustrated in Fig. 1c, PuTR essentially follows the standard architecture of the Transformer [46], composed of a stack of  $N = 6$  identical layers. Each layer has two sub-layers: a masked multi-head self-attention mechanism with 8 heads, and a fully connected feed-forward network. A residual connection is employed around each sub-layer. To improve training stability, we perform layer normalization before each sub-layer input following [6; 45].

The  $\mathcal{S}_{in}$  is fed into PuTR after adding temporal positional encodings, and spatial positional encodings are added before being linearly projected into  $K$  and  $V$  in each attention mechanism. After the  $N$  layers, the output object embeddings are linearly projected into high-dimensional representations, denoted as  $\mathcal{S}_{out} = (\langle \text{bos} \rangle, \mathcal{Z}_{t-T}, \dots, \mathcal{Z}_{t-1}, \mathcal{Z}_t) \in \mathbb{R}^{n_S \times d_{model}}$ , which is then used to calculate the relative affinity matrix between trajectories and current detections to solve the association problem.

**Modifications.** Unlike sentences, object sequences are ordered temporally across frames but unordered spatially within each frame. To account for this, we modify the attention mask and introduce temporal and spatial positional encodings in PuTR.

Since objects in  $\mathcal{O}_t$  are unordered and cannot be interlinked, we modify the conventional causal mask (a lower triangular matrix) to ensure permutation invariance within the same frame. Specifically, based on the causal mask, we additionally set the positions to zero for tokens in the same frame, i.e.,  $mask_{ij} = 0$  if  $t_i == t_j$  &  $i \neq j$ , where  $t_i$  and  $t_j$  are the frame indices of the  $i$ -th and  $j$ -th tokens, respectively. We refer to this as the frame causal mask, which precisely aligns with the distribution of the white blocks in Fig. 1b, and thus consistent with the trajectory graph structure.

For the positional encodings, we adopt the basic absolute positional encoding from the original Transformer [46] to encode the temporal order and the spatial positional encoding from DETR [9] to encode spatial location. Specifically, in  $\mathcal{S}_{in}$ , tokens within  $\mathcal{X}_t$  are added with the same temporal positional encoding before the first layer, indicating their frame order within the current clip (e.g.,  $\mathcal{X}_{t-T}$  has position 0,  $\mathcal{X}_t$  has  $T$ ). Following DETR, the spatial positional encoding concatenates two absolute positional encodings with length  $d_{model}/2$ , representing the object’s center coordinate in the image, and is added to the object embedding before linear projection to  $K$  and  $V$  in each attention mechanism to emphasize the spatial location information, as shown in Fig. 1c.

### 3.3 Training & Inference

**Training.** Unlike language model pre-training, where each output token is required to predict the next word in a fixed vocabulary table via classification, in MOT, the same individual object generates a unique trajectory, making it impractical to establish a fixed individual object vocabulary. While MOTIP [19] proposes using a shared tracking ID dictionary to predict the ID labels of current detected objects, determining the appropriate dictionary size requires empirical tuning for different datasets, and there is a risk of ID exhaustion when the number of tracked objects exceeds the dictionary size.

To ensure generalizability, PuTR circumvents the ID dictionary and instead proposes using the relative affinity matrix to classify the current detected objects, thus accomplishing the association task. Specifically, we calculate the inner product between  $\mathcal{Z}_{t-1}$  and  $\mathcal{Z}_t$ , i.e.,  $\mathcal{Z}_{t-1} \mathcal{Z}_t^\top$  ( $t \geq 1$ ), to obtain the relative affinity matrix, and apply the softmax along rows to obtain the probability distribution of the previous objects corresponding to the next objects. Through the affinity matrix, we can determine the association via the Hungarian algorithm, similar to heuristic methods [4; 57], without the need for a fixed vocabulary table. The classification loss is simply calculated as the cross-entropy loss between the predicted probability and the ground truth label. Thus, without bells and whistles, the training loss of PuTR is straightforwardly calculated as:

$$\mathcal{L} = \frac{\sum_{bs} \sum_T CE(\text{softmax}(\mathcal{Z}_{t-1} \mathcal{Z}_t^\top), Y_t)}{bs \times T}, \quad (1)$$

where  $CE(\cdot)$  denotes the cross-entropy loss,  $Y_t$  is the ground truth label in the  $t$ -th frame, and  $bs$  is the batch size.  $CE(\cdot)$  calculates the cross-entropy loss between the predicted probability and the ground truth label, averaging over the number of objects in  $\mathcal{Z}_{t-1}$ . For a tracking identity  $tid$  in  $\mathcal{Z}_t$  but not in  $\mathcal{Z}_{t-1}$ , we assign the nearest output object embedding with the same  $tid$  before  $\mathcal{Z}_{t-1}$  to calculate the loss, ensuring that each object is supervised during training.

**Inference.** Different methodologies are not opposed to each other. Although DETR-based methods [54; 56; 18; 19] are considered end-to-end, some of them still require a run-time manager to schedule tracklet states and occasionally resolve assignment conflicts between tracklets and detections via heuristic rules or the Hungarian algorithm during inference. From this perspective, they can also be regarded as “Heuristic Methods”, with the distinction that the similarity matrix is generated by neural networks instead of hand-crafted models. Consequently, it is of little surprise that PuTR, as a decoupled method, also requires a run-time manager and the Hungarian algorithm to deal with similar issues during inference.

In the first frame of a video sequence during inference, detected objects with a confidence score greater than  $\tau_{new}$  are recorded as newborn objects and assigned unique tracking identities. At each subsequent time step  $t$ , we first filter the detection results with a confidence threshold  $\tau_{det}$ . These remaining detections are then concatenated with the object sequence  $\mathcal{S}$  from the recent  $T$  frames and fed into PuTR to generate the relative affinity matrix. We then employ the Hungarian algorithm to obtain assignment results and a run-time manager to update the tracklet states. The unmatched object with a detection confidence greater than  $\tau_{new}$  will be considered a newborn target and given a new identity. For more details, please refer to Appendix A.

## 4 Experiments

### 4.1 Settings

**Datasets.** We evaluate PuTR on four MOT datasets: the widely-used DanceTrack [43], MOT17 [32], and MOT20 [12], as well as the recently proposed SportsMOT [11]. DanceTrack and SportsMOT provide large-scale training data, while MOT17 and MOT20 have limited training sequences, comprising seven and four sequences, respectively. Notably, DanceTrack and SportsMOT include official validation sets, enabling exploratory experiments.

**Metrics.** We employ three widely-used metrics: HOTA [29], IDF1 [37], and MOTA [3]. MOTA measures object coverage, while IDF1 focuses on identity preservation. HOTA strikes a balance between these two aspects, as illustrated in Figure 1 of [29]. In the decoupled setting, where all methods are evaluated on the same detection results, MOTA values are nearly identical across different methods. However, HOTA and especially IDF1 can better reflect the performance of the association component. Therefore, we primarily focus on IDF1 and HOTA in our experiments when evaluated on the same detections.

**Implementation Details.** PuTR is implemented using PyTorch, and both training and inference are conducted on a single NVIDIA RTX 4090 GPU. During training, consistent settings are maintained across all datasets for simplicity, although further fine-tuning of hyperparameters could potentially improve performance. PuTR is optimized using the AdamW optimizer and a cosine learning rate schedule with a batch size of 4 for 7 epochs on the corresponding training set. The length of training clips is progressively increased from 4 to 8, 16, 32, 64, and 128 at the 2-nd, 3-rd, 4-th, 5-th, and 6-th epoch, respectively, except on MOT20, where the clip length stays at 64 after the 6-th epoch due to GPU memory limitations. The training time for any dataset is less than 1 hour. During inference, we adopt publicly available YOLOX detections for a fair comparison, as previous works [57; 43; 11]. The number of consecutive frames  $T$  is set to 30 for DanceTrack, SportsMOT, and MOT20, while for MOT17, it is 25 empirically. Hyperparameters are consistent within the same dataset and not specifically tuned for each test sequence. Please refer to the Appendix B for more details.

### 4.2 Comparison with Existing Foundational Online Methods

Tab. 1 compares PuTR with previous foundational online methods on four datasets. As a decoupled method, we primarily focus on the association performance (IDF1 and HOTA) under the same detection results and the generalizability across datasets (domain shift test).

**Comparison with Heuristic Methods.** Regarding association performance across different datasets, the pioneering MOT17 and MOT20 benchmarks have established a solid foundation for the MOT task. However, their limited test sequences (7 and 4, respectively) often lead to sequence-specific hyperparameter tuning by many methods [57; 8] to achieve better performance, potentially distorting the assessment values. In contrast, more recent large-scale datasets like DanceTrack and SportsMOT provide massive test sequences (35 and 150, respectively), making such sequence-specific tuning impractical. Therefore, drawing conclusions about a method’s general association performance should rely on a synthesis of assessments across datasets, especially large-scale ones.

Table 1: Comparison with existing foundational online methods. Higher scores indicate better performance for the IDF1 (I $\uparrow$ ), HOTA (H $\uparrow$ ), and MOTA (M $\uparrow$ ) metrics. Superscripts of other methods denote the publisher, while subscripts specify the base detector employed. **Blue backgrounds** highlight decoupled methods utilizing the same detection results, with best scores in **bold**. The domain shift test assesses PuTR’s generalizability across datasets, where the subscript indicates the training set, and  $\Delta_{max}$  represents the maximum performance gap across the four test sets.

Method	Dancetrack test			SportsMOT test			MOT17 test			MOT20 test		
	I $\uparrow$	H $\uparrow$	M $\uparrow$	I $\uparrow$	H $\uparrow$	M $\uparrow$	I $\uparrow$	H $\uparrow$	M $\uparrow$	I $\uparrow$	H $\uparrow$	M $\uparrow$
<i>Detector-based:</i>												
Tracktor++ [2] <sup>ICCV’19</sup>	-	-	-	-	-	-	52.3	42.1	53.5	-	-	-
CenterTrack [59] <sup>ECCV’20</sup>	35.7	41.8	86.8	60.0	62.7	90.8	64.7	52.2	67.8	-	-	-
FairMOT [58] <sup>JCV’21</sup>	40.8	39.7	82.2	53.5	49.3	86.4	72.3	59.3	73.7	67.3	54.6	61.8
QDTrack [33] <sup>CVPR’21</sup>	44.8	45.7	83.0	62.3	60.4	90.1	66.3	53.9	68.7	-	-	-
TrackFormer [31] <sup>CVPR’22</sup>	-	-	-	-	-	-	68.0	57.3	74.1	65.7	54.7	68.6
MOTR [54] <sup>ECCV’22</sup>	51.5	54.2	79.7	-	-	-	68.4	57.2	71.9	-	-	-
MOTIP [19] <sup>arXiv’24</sup>	72.2	67.5	90.3	75.0	71.9	92.9	71.2	59.2	75.5	-	-	-
<i>Heuristic:</i>												
SORT [4] <sup>ICIP’16</sup>	50.8	47.9	91.8	-	-	-	<b>78.2</b>	63.0	80.1	-	-	-
DeepSORT [49] <sup>ICIP’17</sup>	47.9	45.6	87.8	-	-	-	74.5	61.2	78.0	69.6	57.1	71.8
ByteTrack [57] <sup>ECCV’22</sup>	53.9	47.7	89.6	71.4	64.1	95.9	77.3	63.1	<b>80.3</b>	75.2	61.3	<b>77.8</b>
OC-SORT [8] <sup>CVPR’23</sup>	54.6	55.1	<b>92.0</b>	74.0	73.7	96.5	77.5	<b>63.2</b>	78.0	<b>75.9</b>	<b>62.1</b>	75.5
PuTR (Ours)	<b>58.2</b>	<b>55.8</b>	91.9	<b>75.9</b>	<b>74.9</b>	<b>97.0</b>	74.9	61.7	78.5	74.1	61.1	74.8
<i>Domain shift test:</i>												
PuTR <sub>MOT17</sub>	57.3	55.9	91.7	73.2	73.1	96.8	74.9	61.7	78.5	74.0	60.9	75.2
PuTR <sub>MOT20</sub>	57.4	55.8	91.6	73.7	73.3	96.9	73.9	61.1	78.5	74.1	61.1	74.8
PuTR <sub>DanceTrack</sub>	58.2	55.8	91.9	73.3	72.6	96.9	74.3	61.3	78.7	73.8	60.9	75.1
PuTR <sub>SportsMOT</sub>	58.8	56.5	91.8	75.9	74.9	97.0	74.1	61.3	78.6	73.9	60.9	75.0
$\Delta_{max}$	1.5	0.7	0.3	2.7	2.3	0.2	0.8	0.6	0.2	0.3	0.2	0.4

In PuTR, we maintain consistent hyperparameters within each test set without sequence-specific tuning. Under this setting, PuTR achieves the highest IDF1 and HOTA scores on the large-scale DanceTrack and SportsMOT<sup>2</sup> datasets and exhibits competitive performance on the smaller MOT17 and MOT20 benchmarks. Unlike other methods [57; 8] that perform better on small datasets than large ones, we can reasonably conclude that PuTR, as a new approach, demonstrates solid association ability across diverse scenarios compared to foundational heuristic methods.

Furthermore, by leveraging a pure Transformer to handle various associations uniformly, PuTR is liberated from hand-crafted rules and does not require explicit consideration of challenging factors such as complex non-linear motion [25], low frame rates [28], or camera motion [52], which are essential for heuristic methods. This is particularly evident on DanceTrack, where dancers exhibit complex interactions and non-linear motions, and PuTR maintains a better IDF1 score than the second-best OC-SORT (58.2% vs. 54.6%) due to its long-range dependency modeling capability (see visualizations in Appendix C). These results indicate that PuTR explores a promising new direction for the association problem in the decoupled and online manner.

**Comparison with Detector-based Methods.** PuTR outperforms the representative JDE [58; 33], CNN-based [2; 59], and DETR-based [54; 18] methods on all benchmarks, except the latest DETR-based approach MOTIP [19], warranting a detailed analysis. MOTIP leverages its methodology’s advantages but requires additional training data and substantial computational resources (typically 8 GPUs for days) to achieve satisfactory performance, hence excelling on DanceTrack and SportsMOT. For MOT17, the CrowdHuman [42] dataset, containing massive human images, is incorporated following prior work [54; 18] to mitigate overfitting, improving performance while increasing training complexity. For MOT20, where the average pedestrian count per frame exceeds DETR’s detection capacity, only the early TrackFormer [31] is evaluated by modifying Deformable-DETR, while later incremental works focus on datasets with more moderate object query numbers. In

<sup>2</sup>For SportsMOT, we use the same detection results as ByteTrack and OC-SORT following the Train+Val setup, referring to Table 3 in [11]. In the Train setup, PuTR’s I $\uparrow$ , H $\uparrow$ , M $\uparrow$  are 74.2%, 73.0%, 95.1%, respectively.

contrast, PuTR performs streamlined training from scratch on a single GPU in under 1 hour<sup>3</sup> without any additional data or pretraining, regardless of dataset scale or object count.

On large-scale datasets, PuTR surpasses MOTIP on SportsMOT, while leaving room for improvement on DanceTrack. This is attributed to the complexity of dancer interactions, where YOLOX generates more False Positives (FPs) on DanceTrack than SportsMOT. Through end-to-end learning, MOTIP can detect interacting dancers more precisely under tracking guidance, thus addressing DanceTrack’s most challenging aspect. This indicates that no methodology can perfectly handle all MOT challenges, necessitating a balanced approach. Consequently, PuTR excels on SportsMOT with simple training and precise detection, while even MOTIP with additional image data cannot outperform PuTR on MOT17. Furthermore, PuTR can be easily extended to the dense MOT20 dataset.

Through the aforementioned comparisons, PuTR demonstrates a strong baseline for this emerging direction. Although a performance gap exists between PuTR and the latest incremental methods, the analysis indicates the promising potential of leveraging Transformers for MOT in an alternative way.

**Inference Efficiency.** In addition to training efficiency, PuTR demonstrates remarkable inference speed. Unlike MOTIP’s 22 FPS<sup>4</sup> on DanceTrack, SportsMOT, and MOT17, PuTR can process video sequences at a much higher frame rate due to its relatively simple architecture. Specifically, PuTR’s average FPS on the sparse DanceTrack, SportsMOT, and MOT17 datasets are 89, 92, and 73, respectively. Even on the dense MOT20 dataset, it can still achieve an impressive 27 FPS. While the massive number of tracked objects per frame in MOT20 can lengthen the input object sequence and consequently slow down the speed, it still meets real-time requirements. Moreover, the decoupled approach offers the advantage of independent execution for detection and association, enabling parallel processing pipelines for further efficiency enhancement.

**Generalizability.** Robust association ability across various scenarios is crucial for MOT methods. Heuristic methods can tune hyperparameters to adapt to most common cases, while other learning-based methods rarely report generalizability across datasets despite the urge to address this issue. Only the work [41] addresses the domain adaptation problem in MOT, reporting that QDTrack [33] exhibits a striking degradation, decreasing by 49% in IDF1 and 35% in HOTA when evaluated on DanceTrack with weights trained on MOT17. We also evaluate the official MOTIP weights trained on MOT17 on the DanceTrack test set, only yielding 44.9% IDF1 and 43.0% HOTA.

In contrast, from the domain shift test, we find that PuTR has excellent generalizability across domains. Without any other operation, just applying the weights trained on one dataset to another, the maximum cross-dataset gap is only 2.7% in IDF1 and 2.3% in HOTA, which has never been reported in previous learning-based works. This property of PuTR can be attributed to the fact that it takes advantage of different methodologies, which is appropriate in terms of methodological cross-pollination and integration. It is the decoupled manner that PuTR can obtain precise detection results like heuristic methods, and the self-attention mechanism of the Transformer that can discriminate individuals in the feature space, even in scenes that have never been trained. Furthermore, the relative affinity matrix also plays a crucial role, as it circumvents concerns regarding the dictionary capacity or the exhaustion issue in MOTIP. This property makes the new direction we proposed ever more fascinating, and we believe it will attract more attention in the future and promote a new development in the MOT field. We also report the combined training performance in Appendix D.

### 4.3 Ablation Studies

We conduct ablation studies on the DanceTrack and SportsMOT datasets due to their large-scale training data and availability of official validation sets. More studies are presented in Appendix E.

**Attention Mask.** The attention mask plays a crucial role in enabling the Transformer to capture dependencies between tokens. We evaluate the impact of our proposed frame causal mask compared to the conventional causal mask, and the results are presented in Tab. 2. The models are trained and inferred using the same mask type, and during inference, the shuffle operation randomly shuffles the object order within one frame. Without shuffling, we find that the IDF1 scores of the frame causal mask are 0.2% and 0.5% higher on the DanceTrack and SportsMOT validation sets, respectively, compared to the conventional causal mask (the first and third rows). Although the increase is not significant, the two types of masks are fundamentally different.

<sup>3</sup>Specifically, training time on DanceTrack, SportsMOT, MOT17, and MOT20 is 55, 35, 20, and 20 minutes.

<sup>4</sup>We test the official model’s speed on the same machine as PuTR and exceed the original 16 FPS report.

Table 2: Ablations on the attention mask.

PuTR		Dancetrack val			SportsMOT val		
Mask Type	Shuffle	I↑	H↑	M↑	I↑	H↑	M↑
frame causal		<b>55.7</b>	<b>54.5</b>	<b>88.3</b>	<b>78.6</b>	<b>76.4</b>	<b>95.7</b>
frame causal	✓	55.7	54.5	88.3	78.6	76.4	95.7
causal		55.5	54.4	88.3	78.1	76.1	95.6
causal	✓	54.9	53.6	88.2	77.9	76.0	95.6

Table 3: Ablations on the positional encoding.

Positional Encoding		Dancetrack val			SportsMOT val		
Temporal	Spatial	I↑	H↑	M↑	I↑	H↑	M↑
		55.0	53.9	88.1	78.0	76.3	95.6
✓		55.2	54.3	88.1	78.2	76.4	95.6
✓	✓	<b>55.7</b>	<b>54.5</b>	<b>88.2</b>	<b>78.6</b>	<b>76.4</b>	<b>95.7</b>

Our frame causal mask ensures permutation invariance of objects within the same frame, thereby maintaining consistency between the trajectory graph and the Transformer, i.e., all objects in the same frame are concurrent and cannot associate with each other. Consequently, even when the object order in the frame is randomly shuffled (the second row), the performance remains consistent. In contrast, the causal mask does not possess this property, and the model’s performance is coupled with the training object order, leading to unpredictable results when shuffling (the fourth row).

**Positional Encoding.** Our model incorporates spatial and temporal positional encodings to adjust to the unique characteristics of the object sequence. We experiment with several combinations of these encodings, and the results are presented in Tab. 3. Without these two positional encodings (the first row), the model still achieves reasonably high IDF1 scores of 55.0% and 78.0% on the respective validation sets, losing only 0.7% and 0.6% compared to the complete model (the third row). Introducing the temporal positional encoding leads to a 0.2% increase in IDF1 on both sets (the second row). Since the frame causal mask ensures the correct frame order, temporal positional encodings are not strictly necessary for identifying the frame order, thus leading to a minor improvement. Incorporating the spatial positional encodings into PuTR additionally resulted in an increase of 0.5% and 0.4% in IDF1, respectively. This suggests that even without spatial positional encodings, PuTR could recognize the same individual object based solely on appearance cues, and the spatial positional encodings further enhance this ability by encoding the spatial location in the image.

Overall, even without these modifications, the model still achieves a strong baseline, indicating our proposed approach naturally matches the association problem of MOT.

## 5 Conclusion & Impacts

**Conclusion.** Starting from a trajectory graph, we propose a straightforward approach to model the association problem with a pure Transformer in a decoupled and online fashion. We introduce PuTR to identify challenges in this new direction, establishing a strong baseline compared to existing foundational methods based on other methodologies. We find that the Transformer naturally aligns with this problem, and the decoupled manner enables efficient training and inference while achieving strong generalization across diverse domains. Additionally, we present new perspectives on the relationships among different methodologies, stimulating beneficial cross-pollination and integration while considering the requirements and needs of each other.

**Impacts.** Our work primarily focuses on the conceptual contribution of developing a solution via a pure Transformer architecture, demonstrating the feasibility of this direction for association. Through releasing our code, we aim to inspire and facilitate further research in this promising new paradigm, paving the way for more powerful and efficient MOT solutions. Furthermore, we outline potential future directions:

**Context length.** The context length of the Transformer is a critical factor influencing model performance. In our work, we set the context length to 30 frames in most cases. However, as shown in Appendix E, simply increasing the context length does not consistently yield benefits. Future work could leverage advancements in long context modeling techniques from the language model domain to specifically address this challenge.

**Motion cues.** Although PuTR primarily focuses on appearance cues for re-identification, incorporating motion cues into the Transformer may further enhance performance, particularly in challenging scenarios involving tiny objects, as observed in MOT17 (Appendix F).

Overall, this work pioneers another innovative Transformer-based direction for MOT. The self-attention-driven modeling of trajectories showcased in PuTR opens up exciting possibilities for further advancements in this crucial computer vision task.

## References

- [1] Nir Aharon, Roy Orfaig, and Ben-Zion Bobrovsky. Bot-sort: Robust associations multi-pedestrian tracking. arXiv preprint arXiv:2206.14651, 2022.
- [2] Philipp Bergmann, Tim Meinhardt, and Laura Leal-Taixé. Tracking without bells and whistles. In Proceedings of the IEEE/CVF international conference on computer vision, pages 941–951, 2019.
- [3] Keni Bernardin and Rainer Stiefelhausen. Evaluating multiple object tracking performance: the clear mot metrics. EURASIP Journal on Image and Video Processing, 2008:1–10, 2008.
- [4] Alex Bewley, Zongyuan Ge, Lionel Ott, Fabio Ramos, and Ben Upcroft. Simple online and realtime tracking. In 2016 IEEE international conference on image processing (ICIP), pages 3464–3468. IEEE, 2016.
- [5] Guillem Brasó and Laura Leal-Taixé. Learning a neural solver for multiple object tracking. In Proceedings of the IEEE/CVF conference on computer vision and pattern recognition, pages 6247–6257, 2020.
- [6] Tom Brown, Benjamin Mann, Nick Ryder, Melanie Subbiah, Jared D Kaplan, Prafulla Dhariwal, Arvind Neelakantan, Pranav Shyam, Girish Sastry, Amanda Askell, et al. Language models are few-shot learners. Advances in neural information processing systems, 33:1877–1901, 2020.
- [7] Jiarui Cai, Mingze Xu, Wei Li, Yuanjun Xiong, Wei Xia, Zhuowen Tu, and Stefano Soatto. Memot: Multi-object tracking with memory. In Proceedings of the IEEE/CVF Conference on Computer Vision and Pattern Recognition, pages 8090–8100, 2022.
- [8] Jinkun Cao, Jiangmiao Pang, Xinshuo Weng, Rawal Khrodar, and Kris Kitani. Observation-centric sort: Rethinking sort for robust multi-object tracking. In Proceedings of the IEEE/CVF conference on computer vision and pattern recognition, pages 9686–9696, 2023.
- [9] Nicolas Carion, Francisco Massa, Gabriel Synnaeve, Nicolas Usunier, Alexander Kirillov, and Sergey Zagoruyko. End-to-end object detection with transformers. In European conference on computer vision, pages 213–229. Springer, 2020.
- [10] Orcun Cetintas, Guillem Brasó, and Laura Leal-Taixé. Unifying short and long-term tracking with graph hierarchies. In Proceedings of the IEEE/CVF Conference on Computer Vision and Pattern Recognition, pages 22877–22887, 2023.
- [11] Yutao Cui, Chenkai Zeng, Xiaoyu Zhao, Yichun Yang, Gangshan Wu, and Limin Wang. Sportsmot: A large multi-object tracking dataset in multiple sports scenes. In Proceedings of the IEEE/CVF International Conference on Computer Vision, pages 9921–9931, 2023.
- [12] Patrick Dendorfer, Hamid Rezatofighi, Anton Milan, Javen Shi, Daniel Cremers, Ian Reid, Stefan Roth, Konrad Schindler, and Laura Leal-Taixé. Mot20: A benchmark for multi object tracking in crowded scenes. arXiv preprint arXiv:2003.09003, 2020.
- [13] Patrick Dendorfer, Vladimir Yugay, Aljosa Osep, and Laura Leal-Taixé. Quo vadis: Is trajectory forecasting the key towards long-term multi-object tracking? Advances in Neural Information Processing Systems, 35:15657–15671, 2022.
- [14] Alexey Dosovitskiy, Lucas Beyer, Alexander Kolesnikov, Dirk Weissenborn, Xiaohua Zhai, Thomas Unterthiner, Mostafa Dehghani, Matthias Minderer, Georg Heigold, Sylvain Gelly, Jakob Uszkoreit, and Neil Houlsby. An image is worth 16x16 words: Transformers for image recognition at scale. In International Conference on Learning Representations, 2021.
- [15] Yunhao Du, Zhicheng Zhao, Yang Song, Yanyun Zhao, Fei Su, Tao Gong, and Hongying Meng. Strongsort: Make deepsort great again. IEEE Transactions on Multimedia, 2023.
- [16] Mohamed Elhoseny. Multi-object detection and tracking (modt) machine learning model for real-time video surveillance systems. Circuits, Systems, and Signal Processing, 39(2):611–630, 2020.
- [17] Andreas Ess, Konrad Schindler, Bastian Leibe, and Luc Van Gool. Object detection and tracking for autonomous navigation in dynamic environments. The International Journal of Robotics Research, 29(14):1707–1725, 2010.
- [18] Ruopeng Gao and Limin Wang. Memotr: Long-term memory-augmented transformer for multi-object tracking. In Proceedings of the IEEE/CVF International Conference on Computer Vision, pages 9901–9910, 2023.

- [19] Ruopeng Gao, Yijun Zhang, and Limin Wang. Multiple object tracking as id prediction. arXiv preprint arXiv:2403.16848, 2024.
- [20] Zheng Ge, Songtao Liu, Feng Wang, Zeming Li, and Jian Sun. Yolox: Exceeding yolo series in 2021. arXiv preprint arXiv:2107.08430, 2021.
- [21] Weiming Hu, Tieniu Tan, Liang Wang, and Steve Maybank. A survey on visual surveillance of object motion and behaviors. IEEE Transactions on Systems, Man, and Cybernetics, Part C (Applications and Reviews), 34(3):334–352, 2004.
- [22] Hao Jiang, Sidney Fels, and James J Little. A linear programming approach for multiple object tracking. In 2007 IEEE Conference on Computer Vision and Pattern Recognition, pages 1–8. IEEE, 2007.
- [23] R. E. Kalman. A New Approach to Linear Filtering and Prediction Problems. Journal of Basic Engineering, 82(1):35–45, 03 1960.
- [24] Harold W Kuhn. The hungarian method for the assignment problem. Naval research logistics quarterly, 2(1-2):83–97, 1955.
- [25] Chongwei Liu, Haojie Li, and Zhihui Wang. Fasttrack: A highly efficient and generic gpu-based multi-object tracking method with parallel kalman filter. International Journal of Computer Vision, pages 1–21, 2023.
- [26] Kai Liu, Sheng Jin, Zhihang Fu, Ze Chen, Rongxin Jiang, and Jieping Ye. Uncertainty-aware unsupervised multi-object tracking. In Proceedings of the IEEE/CVF International Conference on Computer Vision, pages 9996–10005, 2023.
- [27] Shilong Liu, Feng Li, Hao Zhang, Xiao Yang, Xianbiao Qi, Hang Su, Jun Zhu, and Lei Zhang. DAB-DETR: Dynamic anchor boxes are better queries for DETR. In International Conference on Learning Representations, 2022.
- [28] Y. Liu, J. Wu, and Y. Fu. Collaborative tracking learning for frame-rate-insensitive multi-object tracking. In 2023 IEEE/CVF International Conference on Computer Vision (ICCV), pages 9930–9939, Los Alamitos, CA, USA, oct 2023. IEEE Computer Society.
- [29] Jonathon Luiten, Aljosa Osep, Patrick Dendorfer, Philip Torr, Andreas Geiger, Laura Leal-Taixé, and Bastian Leibe. Hota: A higher order metric for evaluating multi-object tracking. International journal of computer vision, 129:548–578, 2021.
- [30] Gerard Maggolino, Adnan Ahmad, Jinkun Cao, and Kris Kitani. Deep oc-sort: Multi-pedestrian tracking by adaptive re-identification. In 2023 IEEE International Conference on Image Processing (ICIP), pages 3025–3029. IEEE, 2023.
- [31] Tim Meinhardt, Alexander Kirillov, Laura Leal-Taixe, and Christoph Feichtenhofer. Trackformer: Multi-object tracking with transformers. In Proceedings of the IEEE/CVF conference on computer vision and pattern recognition, pages 8844–8854, 2022.
- [32] Anton Milan, Laura Leal-Taixé, Ian Reid, Stefan Roth, and Konrad Schindler. Mot16: A benchmark for multi-object tracking. arXiv preprint arXiv:1603.00831, 2016.
- [33] Jiangmiao Pang, Linlu Qiu, Xia Li, Haofeng Chen, Qi Li, Trevor Darrell, and Fisher Yu. Quasi-dense similarity learning for multiple object tracking. In Proceedings of the IEEE/CVF conference on computer vision and pattern recognition, pages 164–173, 2021.
- [34] Hamed Pirsiavash, Deva Ramanan, and Charless C. Fowlkes. Globally-optimal greedy algorithms for tracking a variable number of objects. In CVPR 2011, pages 1201–1208, 2011.
- [35] Joseph Redmon and Ali Farhadi. Yolov3: An incremental improvement. arXiv preprint arXiv:1804.02767, 2018.
- [36] Shaoqing Ren, Kaiming He, Ross Girshick, and Jian Sun. Faster r-cnn: Towards real-time object detection with region proposal networks. Advances in neural information processing systems, 28, 2015.
- [37] Ergys Ristani, Francesco Solera, Roger Zou, Rita Cucchiara, and Carlo Tomasi. Performance measures and a data set for multi-target, multi-camera tracking. In European conference on computer vision, pages 17–35. Springer, 2016.

- [38] Amir Roshan Zamir, Afshin Dehghan, and Mubarak Shah. Gmcp-tracker: Global multi-object tracking using generalized minimum clique graphs. In Computer Vision–ECCV 2012: 12th European Conference on Computer Vision, Florence, Italy, October 7–13, 2012, Proceedings, Part II 12, pages 343–356. Springer, 2012.
- [39] David E Rumelhart, Geoffrey E Hinton, and Ronald J Williams. Learning representations by back-propagating errors. nature, 323(6088):533–536, 1986.
- [40] Franco Scarselli, Marco Gori, Ah Chung Tsoi, Markus Hagenbuchner, and Gabriele Monfardini. The graph neural network model. IEEE transactions on neural networks, 20(1):61–80, 2008.
- [41] Mattia Segu, Bernt Schiele, and Fisher Yu. Darth: Holistic test-time adaptation for multiple object tracking. In Proceedings of the IEEE/CVF International Conference on Computer Vision, pages 9717–9727, 2023.
- [42] Shuai Shao, Zijian Zhao, Boxun Li, Tete Xiao, Gang Yu, Xiangyu Zhang, and Jian Sun. Crowdhuman: A benchmark for detecting human in a crowd. arXiv preprint arXiv:1805.00123, 2018.
- [43] Peize Sun, Jinkun Cao, Yi Jiang, Zehuan Yuan, Song Bai, Kris Kitani, and Ping Luo. Dancetrack: Multi-object tracking in uniform appearance and diverse motion. In Proceedings of the IEEE/CVF Conference on Computer Vision and Pattern Recognition, pages 20993–21002, 2022.
- [44] Siyu Tang, Mykhaylo Andriluka, Bjoern Andres, and Bernt Schiele. Multiple people tracking by lifted multicut and person re-identification. In Proceedings of the IEEE conference on computer vision and pattern recognition, pages 3539–3548, 2017.
- [45] Hugo Touvron, Louis Martin, Kevin Stone, Peter Albert, Amjad Almahairi, Yasmine Babaei, Nikolay Bashlykov, Soumya Batra, Prajjwal Bhargava, Shruti Bhosale, et al. Llama 2: Open foundation and fine-tuned chat models. arXiv preprint arXiv:2307.09288, 2023.
- [46] Ashish Vaswani, Noam Shazeer, Niki Parmar, Jakob Uszkoreit, Llion Jones, Aidan N Gomez, Łukasz Kaiser, and Illia Polosukhin. Attention is all you need. Advances in neural information processing systems, 30, 2017.
- [47] Shuai Wang, Da Yang, Yubin Wu, Yang Liu, and Hao Sheng. Tracking game: Self-adaptive agent based multi-object tracking. In Proceedings of the 30th ACM International Conference on Multimedia, pages 1964–1972, 2022.
- [48] Zhongdao Wang, Liang Zheng, Yixuan Liu, Yali Li, and Shengjin Wang. Towards real-time multi-object tracking. In European conference on computer vision, pages 107–122. Springer, 2020.
- [49] Nicolai Wojke, Alex Bewley, and Dietrich Paulus. Simple online and realtime tracking with a deep association metric. In 2017 IEEE international conference on image processing (ICIP), pages 3645–3649. IEEE, 2017.
- [50] Feng Yan, Weixin Luo, Yujie Zhong, Yiyang Gan, and Lin Ma. Bridging the gap between end-to-end and non-end-to-end multi-object tracking. arXiv preprint arXiv:2305.12724, 2023.
- [51] Mingzhan Yang, Guangxin Han, Bin Yan, Wenhua Zhang, Jinqing Qi, Huchuan Lu, and Dong Wang. Hybrid-sort: Weak cues matter for online multi-object tracking. In Proceedings of the AAAI Conference on Artificial Intelligence, volume 38, pages 6504–6512, 2024.
- [52] Kefu Yi, Kai Luo, Xiaolei Luo, Jiangui Huang, Hao Wu, Rongdong Hu, and Wei Hao. Ucmctrack: Multi-object tracking with uniform camera motion compensation. In Proceedings of the AAAI Conference on Artificial Intelligence, volume 38, pages 6702–6710, 2024.
- [53] En Yu, Tiancai Wang, Zhuoling Li, Yang Zhang, Xiangyu Zhang, and Wenbing Tao. Motrv3: Release-fetch supervision for end-to-end multi-object tracking. arXiv preprint arXiv:2305.14298, 2023.
- [54] Fangao Zeng, Bin Dong, Yang Zhang, Tiancai Wang, Xiangyu Zhang, and Yichen Wei. Motr: End-to-end multiple-object tracking with transformer. In European Conference on Computer Vision, pages 659–675. Springer, 2022.
- [55] Li Zhang, Yuan Li, and Ramakant Nevatia. Global data association for multi-object tracking using network flows. In 2008 IEEE conference on computer vision and pattern recognition, pages 1–8. IEEE, 2008.
- [56] Y. Zhang, T. Wang, and X. Zhang. Motrv2: Bootstrapping end-to-end multi-object tracking by pretrained object detectors. In 2023 IEEE/CVF Conference on Computer Vision and Pattern Recognition (CVPR), pages 22056–22065, Los Alamitos, CA, USA, jun 2023. IEEE Computer Society.

- [57] Yifu Zhang, Peize Sun, Yi Jiang, Dongdong Yu, Fucheng Weng, Zehuan Yuan, Ping Luo, Wenyu Liu, and Xinggang Wang. Bytetrack: Multi-object tracking by associating every detection box. In European conference on computer vision, pages 1–21. Springer, 2022.
- [58] Yifu Zhang, Chunyu Wang, Xinggang Wang, Wenjun Zeng, and Wenyu Liu. Fairmot: On the fairness of detection and re-identification in multiple object tracking. International Journal of Computer Vision, 129:3069–3087, 2021.
- [59] Xingyi Zhou, Vladlen Koltun, and Philipp Krähenbühl. Tracking objects as points. In European conference on computer vision, pages 474–490. Springer, 2020.
- [60] Xingyi Zhou, Dequan Wang, and Philipp Krähenbühl. Objects as points. arXiv preprint arXiv:1904.07850, 2019.
- [61] Xizhou Zhu, Weijie Su, Lewei Lu, Bin Li, Xiaogang Wang, and Jifeng Dai. Deformable DETR: Deformable transformers for end-to-end object detection. In International Conference on Learning Representations, 2021.

# Appendix

The appendix complements our work with additional information on inference pipeline in Appendix A. Furthermore, we provide more experiment details in Appendix B, and visual results in Appendix C. We also conduct additional experiments in Appendix D and E. Finally, we analyze the failure case in Appendix F.

## A Inference Pipeline.

---

**Algorithm 1** Inference pipeline.

---

**Require:** A video sequence  $\mathcal{V}$ ; a detector  $Det(\cdot)$ ; a lost tolerance  $T$ .

```

1: The set of trajectories  $\mathcal{T}^* \leftarrow \emptyset$ ; The set of active trajectories  $\mathcal{T}_{active}^* \leftarrow \emptyset$ .
2: for  $frame_t$  in  $\mathcal{V}$  do
  /* generate detected objects */
3:    $\mathcal{O}_t \leftarrow Det(frame_t)$ ;
  /* generate an affinity matrix */
4:    $\mathbf{A} \leftarrow GenAffinity(\mathcal{T}_{active}^*, \mathcal{O}_t)$ ;
  /* associate */
5:    $\mathcal{O}_m, \mathcal{T}_m^*, \mathcal{O}_u, \mathcal{T}_u^* \leftarrow Hungarian(\mathbf{A})$ 
6:    $\mathcal{O}_m$ : matched detections from  $\mathcal{O}_t$ ;
7:    $\mathcal{T}_m^*$ : matched tracklets from  $\mathcal{T}_{active}^*$ ;
8:    $\mathcal{O}_u$ : unmatched detections from  $\mathcal{O}_t$ ;
9:    $\mathcal{T}_u^*$ : unmatched tracklets from  $\mathcal{T}_{active}^*$ ;
  /* update tracklets */
10:  for  $\mathcal{T}_{tid}, \mathcal{O}_{tid}^t$  in  $\mathcal{T}_m^*, \mathcal{O}_m$  do
11:     $\mathcal{T}_{tid} \leftarrow Update(\mathcal{T}_{tid}, \mathcal{O}_{tid}^t)$ ;
12:  end for
  /* remove tracklets */
13:  for  $\mathcal{T}_{tid}$  in  $\mathcal{T}_u^*$  do
14:    if  $LostGap(\mathcal{T}_{tid}) > T$  or  $\mathcal{T}_{tid}.State == New$  then
15:       $\mathcal{T}_u^* \leftarrow \mathcal{T}_u^* \setminus \{\mathcal{T}_{tid}\}$ ;
16:       $\mathcal{T}^* \leftarrow \mathcal{T}^* \cup \{\mathcal{T}_{tid}\}$ ;
17:    else
18:       $\mathcal{T}_{tid}.State \leftarrow Lost$ ;
19:    end if
20:  end for
21:   $\mathcal{T}_{active}^* \leftarrow \mathcal{T}_m^* \cup \mathcal{T}_u^*$ ;
  /* initialize new tracklets */
22:   $\mathcal{T}_{active}^* \leftarrow \mathcal{T}_{active}^* \cup Init(\mathcal{O}_u)$ ;
23: end for
24:  $\mathcal{T}^* \leftarrow \mathcal{T}^* \cup \mathcal{T}_{active}^*$ ;
Ensure:  $\mathcal{T}^*$ .

```

---

Algo. 1 shows the inference pipeline of our method. The pipeline follows a similar style to heuristic methods, such as ByteTrack [57], while maintaining a concise variant adopted from FastTrack [25], requiring only one association during one frame to avoid increasing complexity. The inputs of the pipeline are a video sequence  $\mathcal{V}$ , a detector  $Det(\cdot)$ , and a lost tolerance  $T$  (same as the input frame length of PuTR). The output is the set of trajectories  $\mathcal{T}^*$ , and we also maintain a set of active trajectories  $\mathcal{T}_{active}^*$  to record the tracklets that are not terminated yet. Each tracklet in  $\mathcal{T}_{active}^*$  has a state attribute, called *State* (one of *Track*, *Lost*, or *New*), to indicate its status at the current frame. For each frame  $frame_t$  in  $\mathcal{V}$ , we obtain the set of detected objects  $\mathcal{O}_t$  via  $Det(\cdot)$  (line 3), filtering by confidence threshold  $\tau_{det}$  and initializing tracking identities  $tid$  to  $-1$ . We then generate a relative affinity matrix using  $\mathcal{T}_{active}^*$  and  $\mathcal{O}_t$  through PuTR as described in the main paper. To enhance tracking performance, we calculate the affinity matrix on the entire output sequence  $S_{out}$  instead of just the last two frames. We first compute a matrix via  $softmax([\mathcal{Z}_{t-T}, \dots, \mathcal{Z}_{t-1}] \mathcal{Z}_t^T)$ , and average the rows with the same  $tid$  as well as incorporate bounding box information as in FastTrack to obtain the robust trajectory-detection relative affinity matrix  $\mathbf{A}$ . The Hungarian algorithm then processes  $\mathbf{A}$  to obtain the assignment results, i.e., matched objects  $\mathcal{O}_m$ , matched tracklets  $\mathcal{T}_m^*$ , unmatched detections  $\mathcal{O}_u$ , and unmatched tracklets  $\mathcal{T}_u^*$  (lines 4 to 9). The objects in  $\mathcal{O}_m$  will be updated into the corresponding tracklets in  $\mathcal{T}_m^*$  (lines 10 to 12), where the *State* of tracklets will be set to *Track*. Then, the tracklets in  $\mathcal{T}_u^*$  will be moved from  $\mathcal{T}_{active}^*$  into  $\mathcal{T}^*$  if the lost gap is larger than  $T$  or its *State* is *New*, following ByteTrack. Otherwise, they will remain in  $\mathcal{T}_{active}^*$ , and their *State* will be set to *Lost* (lines 13 to 20). Next, objects in  $\mathcal{O}_u$  will be initialized as new tracklets and added into  $\mathcal{T}_{active}^*$  after filtering with the

Table 4: Comparison between the combined and single training on PuTR.

PuTR	Dancetrack test			SportsMOT test			MOT17 test			MOT20 test		
	I↑	H↑	M↑	I↑	H↑	M↑	I↑	H↑	M↑	I↑	H↑	M↑
Combined training	57.0	54.5	91.8	75.0	74.0	97.0	74.7	61.4	78.3	<b>74.3</b>	<b>61.2</b>	<b>75.2</b>
Single training	<b>58.2</b>	<b>55.8</b>	<b>91.9</b>	<b>75.9</b>	<b>74.9</b>	<b>97.0</b>	<b>74.9</b>	<b>61.7</b>	<b>78.5</b>	74.1	61.1	74.8

confidence threshold  $\tau_{new}$  (line 22). Finally, after processing all frames in  $\mathcal{V}$ ,  $\mathcal{T}_{active}^*$  will be merged into  $\mathcal{T}^*$ , and  $\mathcal{T}^*$  is the final tracking result of the video sequence  $\mathcal{V}$  (line 24). Due to space constraints, more specific details about  $GenAffinity(\cdot)$ ,  $Update(\cdot)$ ,  $LostGap(\cdot)$ , and  $Init(\cdot)$  functions cannot be elaborated here. Please refer to our code repository for further information.

## B Experiment Details

This section provides a comprehensive description of the experimental details regarding the training and inference of our proposed PuTR. For more specific details, we kindly refer the readers to our code repository.

**Computational Efficiency.** We leverage the `grid_sample` function<sup>5</sup> to simultaneously sample the grid center points of all objects within a frame. Moreover, the `scaled_dot_product_attention` function<sup>6</sup> is employed to accelerate the calculation of the attention mechanism during both training and inference. Additionally, we implement a run-time manager following FastTrack [25], maintaining active tracklets in a tensor array instead of a list of Python entities, thereby facilitating parallel processing and further improving efficiency.

**Training Details.** During the training phase, the initial learning rate is set to 0.0002. We apply weight decay of 0.0005, gradient clipping of 1.0, and accumulate gradients for 32 steps. Following the practices of previous works [56; 18], training clips are sampled from the training sequences with a random interval ranging from 1 to 10, and augmented with random cropping, random resizing, HSV color jittering, and random horizontal flipping to enhance diversity.

**Inference Details.** In the inference stage, we set the confidence threshold  $\tau_{det}$  to 0.1 across all four datasets. The newborn threshold  $\tau_{new}$  is set to 0.6 for DanceTrack, SportsMOT, and MOT17, and 0.4 for MOT20, generally following the practices of previous works [57; 8].

**Detection Results.** The detection results for DanceTrack are obtained from <https://github.com/DanceTrack/DanceTrack>, for MOT17 and MOT20 from <https://github.com/ifzhang/ByteTrack>, and for SportsMOT from <https://github.com/MCG-NJU/MixSort>.



Figure 2: Visual results of PuTR on the DanceTrack (top row) and the SportsMOT (bottom row), showcasing the model’s capability to handle challenging scenarios such as extended occlusions (the blue arrow), and the individual moving out of and re-entering the camera view (the dark arrow).

## C Visual Results

Fig.2 showcases visual results of PuTR on the DanceTrack and SportsMOT datasets. The top row displays the tracking performance on the `#dancetrack0011` video sequence from DanceTrack, while the bottom row illustrates the tracking results on the `#v_IUDUODIBSc_c004` video sequence from SportsMOT. Leveraging the Transformer’s capability to model long-range dependencies, PuTR can identify individuals even after extended occlusions, without relying on motion cues, as exemplified in the top row of Fig.2. The blue dancer is

<sup>5</sup>`torch.nn.functional.grid_sample`

<sup>6</sup>`torch.nn.functional.scaled_dot_product_attention`

Table 5: Ablations on the structure parameters.

$d_{model}$	layers	Dancetrack val			SportsMOT val		
		I $\uparrow$	H $\uparrow$	M $\uparrow$	I $\uparrow$	H $\uparrow$	M $\uparrow$
256	3	54.3	52.7	88.3	<b>78.7</b>	<b>76.8</b>	<b>95.7</b>
256	6	54.2	52.5	88.3	78.3	76.4	95.7
256	9	54.4	52.5	88.2	78.0	76.0	95.7
512	3	<b>56.1</b>	54.3	<b>88.3</b>	78.4	76.4	95.7
512	6	55.7	<b>54.5</b>	88.2	78.6	76.4	95.7
512	9	54.5	53.8	87.9	76.4	75.0	95.6

Table 6: Ablations on the input frame length.

PuTR	$T$	Dancetrack val				SportsMOT val			
		I $\uparrow$	H $\uparrow$	M $\uparrow$	F $\uparrow$	I $\uparrow$	H $\uparrow$	M $\uparrow$	F $\uparrow$
5	5	54.3	<b>55.5</b>	<b>89.0</b>	<b>91</b>	76.8	75.9	95.6	<b>91</b>
15	15	55.3	54.0	88.7	89	78.7	<b>77.1</b>	<b>95.8</b>	89
30	30	<b>55.7</b>	54.5	88.2	89	78.6	76.4	95.7	88
60	60	53.6	51.7	88.0	86	79.0	76.5	95.6	84
90	90	53.7	51.8	87.7	83	<b>79.3</b>	76.1	95.6	83
120	120	53.9	51.9	87.8	78	77.8	74.8	95.5	77

successfully re-identified after a long-term occlusion and a large position change. Furthermore, the long-range dependency modeling enables PuTR to track individuals that move out of and re-enter the camera view. As depicted in the bottom row of Fig. 2, the dark athlete moves out of the camera view in the third frame due to camera motion and reappears in the fourth frame. In such scenarios, conventional motion estimation methods struggle, whereas PuTR can seamlessly track the individual within a simple Transformer architecture. The above results constantly demonstrate PuTR’s ability to uniformly handle challenging cases under a pure Transformer architecture, indicating the promising potential of this new direction.

## D Combined Training

In this section, we compare the performance of the combined training approach with the single dataset training. The combined training refers to training PuTR on the combined training sets of DanceTrack, SportsMOT, MOT17, and MOT20, while the model is evaluated on the respective test sets. Conversely, the single dataset training is the default training process described in the main paper, where the model is trained on a single training set and evaluated on the corresponding test set. The training process for the combined training is consistent with the single dataset training, and the hyperparameters are kept the same. However, due to GPU memory limitations, the training clip length is fixed at 64 frames after the 6-th epoch, as MOT20 is included in the combination.

As shown in Tab. 4, the combined training approach only yields a slight improvement on the MOT20 dataset, while the performance decreases on the other datasets. This observation suggests that the model trained on the combined datasets does not exhibit a significant advantage over the model trained on a single dataset.

## E More Ablation Studies

In this section, we provide further ablation studies on the DanceTrack and SportsMOT validation datasets, where I $\uparrow$ , H $\uparrow$ , M $\uparrow$ , and F $\uparrow$  denote IDF1, HOTA, MOTA, and FPS, respectively.

**Structure Parameters.** Tab. 5 presents the ablation study on the structure parameters of PuTR. We experiment with different numbers of layers and hidden dimensions  $d_{model}$ . For the DanceTrack dataset, which features similar appearance and complex interactions, PuTR requires more hidden dimensions to distinguish individuals, and the performance improves with 512 dimensions compared to 256 dimensions. For SportsMOT, where athletes are sparsely distributed and have straightforward trajectories, the performance is not significantly affected by the hidden dimensions. Unlike end-to-end methods, PuTR solely focuses on the relatively simple association task. Deep layers can lead to overfitting, consequently decreasing performance, as observed with the 9-layer model compared to the 6-layer model under 512 dimensions. Therefore, we adopt the 6-layer model with 512 hidden dimensions as the default setting to ensure robust performance across diverse datasets.

**Input Frame Length.** Tab. 6 presents the ablation study on the input frame length of PuTR during inference. A consistent observation is that the processing speed decreases with increasing input frame length. From 5 to 120 frames, the speed reduction is approximately 12 FPS on both datasets, while still maintaining a high level. Regarding performance, there is no consistent frame length that achieves the best performance on both datasets. For DanceTrack, 5 frames achieve the best HOTA performance, while for SportsMOT, 90 frames achieve the best IDF1 performance. This indicates that the distribution of lost gaps differs between datasets, and stronger long context modeling techniques are required to specifically address this challenge in future works. In our case, we set the default frame length to 30 to strike a balance between performance and speed across various scenarios.

## F Failure Case

PuTR can re-identify the same object based on appearance cues, even after an extended occlusion period, irrespective of its position change. However, this characteristic also leads to a well-known limitation: the inability to discriminate objects with weak appearance information, a common issue in methods relying on the similarity of appearance features. As illustrated in Fig. 3, we observe that PuTR produces false matches between

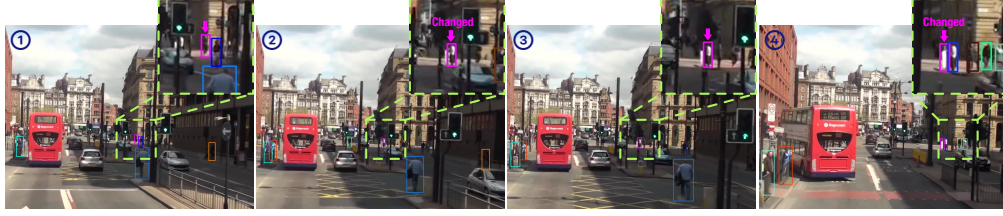


Figure 3: An example of the failure case in video sequence *#MOT17-14*. The tiny pink bounding box changes individuals twice in the second and fourth frame, due to the weak appearance cues.

small objects in the MOT17 dataset, where these objects lack sufficient appearance cues for re-identification. In contrast, from a motion perspective, they are easily distinguishable. To alleviate this issue, future work could encode motion cues into the Transformer to enhance the association performance.